

# Interfacial assembly of dendritic microcapsules with host-guest chemistry

Yu Zheng<sup>a,b,c</sup>, Ziyi Yu<sup>a,c</sup>, Richard M. Parker<sup>c</sup>, Yuchao Wu<sup>b,c</sup>, Chris Abell<sup>c</sup>, and Oren A. Scherman<sup>\*b,c</sup>

<sup>a</sup>Contributed equally to the work

<sup>b</sup>Melville Laboratory for Polymer Synthesis

<sup>c</sup>Department of Chemistry, University of Cambridge, Cambridge, CB2 1EW, United Kingdom

\*e-mail: oas23@cam.ac.uk

October 23, 2014

**The self assembly of nanoscale materials to form hierarchically-ordered structures promises new opportunities in drug delivery, as well as magnetic materials and devices. Herein, we report a simple means to promote the self assembly of two polymers with functional groups at a water-chloroform interface using microfluidic technology. Two polymeric layers can be assembled and dissembled at the droplet interface using the efficiency of cucurbit[8]uril host-guest supramolecular chemistry. The microcapsules produced are extremely monodisperse in size and can encapsulate target molecules in a robust, well-defined manner. Additionally, we exploit a dendritic copolymer architecture to trap a small hydrophilic molecule in the microcapsule skin as cargo. This demonstrates not only the ability to encapsulate small molecules but also the ability to orthogonally store both hydrophilic and hydrophobic cargos within a single microcapsule. The interfacially-assembled supramolecular microcapsules can benefit from the diversity of polymeric materials, allowing for fine control over the microcapsule properties.**

## Introduction

Molecular self assembly is of importance in the fabrication of uniformly-patterned functional surfaces, membranes and delivery vehicles, including hydrogels and microcapsules<sup>1,2</sup>. The self assembly of molecular monolayers can be readily accomplished at a variety of interfaces, including metal (*e.g.* gold), metal oxide substrates (*e.g.* silica) or at an air/water interface, to form self-assembled monolayers<sup>3-6</sup>. More recently, the introduction of compartmentalisation into such complex nano- or micro-scale systems is attracting considerable and wide ranging interest for application in future delivery technologies<sup>7-9</sup>.

Relative to planar interfaces, the spherical surface of a droplet offers improved interaction with the surrounding environment for sensing applications (*e.g.* SERS) or as a means of encapsulating a target cargo for localised study (*e.g.* FRET) or protection (*e.g.* enzymatic catalysis). The development of microfluidic techniques has revolutionised the formation of micro-scale droplets, allowing for high monodispersity in both size and composition, reproducibility, material efficiency and high throughput manipulation and analysis<sup>10,11</sup>. The self assembly of nanoparticles at the droplet interface

between immiscible fluids to form a Pickering emulsion, driven by a reduction in interfacial energy, is well established<sup>12,13</sup>. Progressing to polymer-only materials to form multilayer hollow structures promises new opportunities in drug delivery as well as optical, acoustic, electronic and magnetic materials. However, polymer chain entanglement competes with thermal fluctuations and interfacial energy, giving rise to complicated self assembly behaviour.

To date, several approaches to prepare polymeric microcapsules have been adopted. In addition to self assembled vesicles<sup>14-18</sup> or synthetic polymersomes<sup>19</sup>, the majority of reported structures rely on templating by *exo*-<sup>20-22</sup>, *meso*-<sup>23,24</sup>, *endo*-<sup>25</sup> or *exo-endo*<sup>26,27</sup> methods. These approaches are experimentally laborious, with the use of a solid template requiring subsequent etching under relatively harsh conditions to obtain a hollow structure, lowering encapsulation and loading efficiencies. Droplets-in-droplet based double or multiple emulsion strategies<sup>28,29</sup>, although powerful, depend on ingenious microfluidic devices and considerable interfacial tension between different phases. These assemblies are typically not robust (*e.g.* vesicles that cannot be dried) or more importantly rely on covalent crosslinking to give a microcapsule structure, limiting the opportunities for controlled disassembly required for on-demand release of cargo. While there have been examples of microcapsules formed from interfacial polymerisation<sup>30,31</sup> or cross-linking<sup>32</sup> of monomers at the interface of a microdroplet, the interfacial assembly of pre-formed polymeric materials to form multi-layer amphiphilic microcapsules has not yet been demonstrated.

Supramolecular host-guest chemistry has been applied in the preparation of various self-assembled structures, including polymers<sup>33,34</sup>, micelles<sup>35</sup>, hydrogels<sup>36,37</sup>, colloids<sup>38</sup> and more recently by our group, microcapsules<sup>39</sup>. In this supramolecular system, cucurbit[8]uril (CB[8]) was exploited to crosslink a naphthol-modified poly(acrylamide) copolymer and methyl viologen-functionalised gold nanoparticles, forming a nanocomposite supramolecular skin around aqueous microdroplets. CB[8] is a macrocyclic host molecule that is capable of simultaneously encapsulating two

guests within its cavity, forming a stable yet dynamic ternary complex<sup>40,41</sup>. While we demonstrated a simple one-step approach to supramolecular microcapsules<sup>39</sup>, there were also a few limitations inherent to the system, such as the reliance on metal nanoparticles to direct self assembly and the relatively large pore size preventing encapsulation of small molecules. Initial attempts to replace the metal nanoparticles with polymeric equivalents resulted in all components dispersed throughout the aqueous phase, indicating that a new strategy towards the formation of supramolecular polymer-only microcapsules was required.

Herein, we report the self assembly of

complementary-functionalised hydrophilic and hydrophobic copolymers that can be controllably brought together at the water-chloroform interface of a microfluidic droplet. By forming a robust ternary host-guest complexes with CB[8], these functional copolymers can be reversibly cross-linked to form a polymeric skin at the microdroplet interface, giving rise to a supramolecular polymer-only microcapsule. These template free, interfacially-assembled microcapsules are monodisperse in size and composition, with a high cargo encapsulation efficiency. Furthermore, we improve the efficacy of our microcapsule through the use of a dendritic copolymer. The dendritic nature of

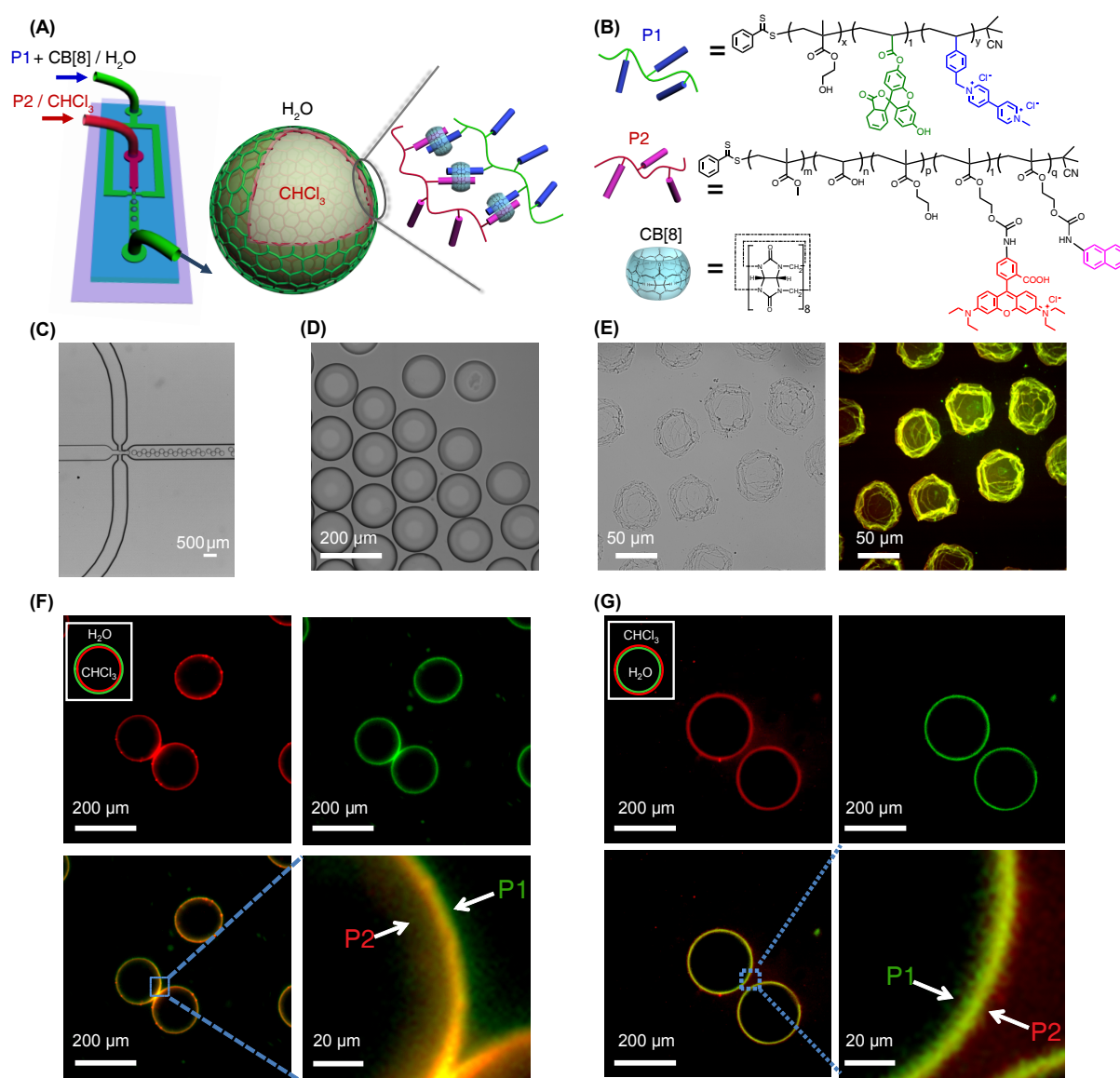


**Figure 1: Supramolecular assembly of microcapsules at the interface of microfluidic droplets.** (a) Schematic representation of the microdroplet generation process using a microfluidic flow focusing device, where an aqueous continuous phase containing CB[8] and copolymer **P1** (functionalised with MV and FOA) intersects an immiscible chloroform phase containing copolymer **P2** (functionalised with Np and Rhodamine B) at a flow focusing microchannel junction to form a periodic flow of oil-in-water microdroplets. (b) The chemical structures of hydrophilic poly(HEMA-co-StMV-co-FOA), **P1**; hydrophobic poly(MMA-co-AA-co-HEMA-NP), **P2**; and CB[8]. (c) Micrograph of oil-in-water microdroplets generated at the microfluidic flow focusing channel junction. (d) The high monodispersity of the formed microdroplets is demonstrated by the narrow size distribution ( $d = 102.4 \pm 0.5 \mu\text{m}$ ). (e) Bright field (left) and fluorescence (right) images of microcapsules formed after evaporation of the chloroform droplet, resulting in a collapsed capsule-like structure. (f) Fluorescence micrographs of the highly monodisperse chloroform-in-water microdroplets demonstrating the interfacial assembly of **P2** (Rhodamine-tagged, red) within the droplet and **P1** (Fluorescein-tagged, green) present in the external media. (g) Fluorescence micrographs of the inverted water-in-chloroform microdroplets illustrating reversal of **P1** and **P2** at the droplet interface.

the functionalised copolymer enables the entrapment of small molecules within the microcapsule skin, demonstrating an additional level of compartmentalisation of hydrophilic cargo (in this case) surrounding the microcapsule's hydrophobic interior<sup>42,43</sup>. The extent of encapsulation by a dendritic copolymer, the ability to incorporate such a structure into the microcapsule skin and the subsequent triggered release of cargo via an external UV stimulus are presented.

## Results

### Interfacial assembly of supramolecular polymer capsules

Supramolecular assembly between two complementary functionalised polymers and CB[8] has been used to form a wide range of polymeric materials<sup>35 44,45</sup>. All of these examples to date, however, have taken place in aqueous media. By limiting each copolymer to distinct and immiscible phases, the assembly process can be restricted exclusively to the liquid-liquid interface, giving rise to a polymer sheet. Furthermore, by restricting the assembly to the spherical interface of a microdroplet a polymer microcapsule can be formed around the droplet, encapsulating its contents. Herein we describe the preparation of microdroplets containing chloroform-in-water to template the interfacial assembly of the supramolecular microcapsules.

A hydrophilic copolymer and CB[8] were dissolved in the aqueous continuous phase while a complementary hydrophobic copolymer was delivered in the chloroform microdroplet. Water soluble poly(HEMA-*co*-StMV-*co*-FOA) (**P1** in Fig. 1b) was synthesised by reversible addition-fragmentation chain-transfer (RAFT) polymerisation containing 20 mol% of MV<sup>2+</sup> groups ( $M_w = 21$  kDa, PDI = 1.3, Supplementary Figure 1). Similarly, the hydrophobic poly(MMA-*co*-AA-*co*-HEMA) was synthesised *via* RAFT copolymerisation ( $M_w = 16$  kDa, PDI = 1.2) and subsequently functionalised with naphthalene isocyanate and Rhodamine B isothiocyanate (**P2** in Fig. 1b and Supplementary Figure 2). Interfacial assembly was accomplished using a microfluidic device comprising two inlets meeting at a single flow focussing junction, as shown in Fig. 1a. To ensure generation of chloroform-in-water microdroplets, the surface of the microchannels were pre-treated with a hydrophilic polyelectrolyte layer. At the microfluidic flow focussing junction the chloroform phase intersects with the perpendicularly-flowing aqueous continuous phase, resulting in droplets of chloroform periodically being sheared (Fig. 1c). With a water:chloroform ratio of flow rates of 2:1, stable microdroplets were generated with a high level of monodispersity, as indicated by the narrow size distribution with a mean diameter of 102.4  $\mu\text{m}$  and a low coefficient of variation of 1.6% (Fig. 1d). CB[8] can form a stable 1:1:1 heteroternary complex with an electron deficient and electron rich guest pair, such as a methyl viologen (MV) and a naphthol (Np) derivative, leading to an overall binding constant ( $K_a$ ) up to  $10^{12}$  M<sup>-2</sup> in water<sup>46</sup>. Here the MV moiety is located on the hydrophilic copolymer **P1**, while Np is found on the hydrophobic copolymer **P2**. The aqueous solution contained 60  $\mu\text{M}$  of the methyl viologen dication (MV<sup>2+</sup>) pendant group

and 60  $\mu\text{M}$  CB[8], while the dispersed phase consisted of a chloroform solution containing 60  $\mu\text{M}$  of naphthalene moieties.

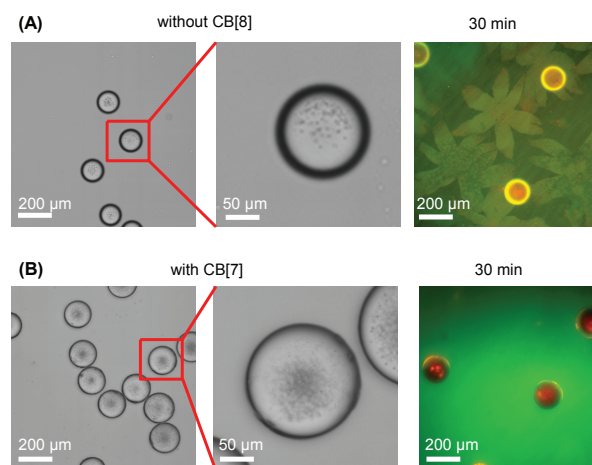


**Figure 2: Confirmation of the role of supramolecular cross-linking in microcapsule formation.** (a) Microdroplets formed in the absence of CB[8] did not lead to the formation of robust microcapsules, any microcapsules that did form were observed to rupture, giving rise to flower-like polymer sheets. (b) Similarly, attempts to form microcapsules *via* CB[7] were unsuccessful, with fluorescence microscopy confirming that copolymers **P1** and **P2** were no longer assembling at the chloroform-water droplet interface, but instead remained dispersed throughout the media.

The heteroternary complex exclusively forms at the interface of the microdroplet between **P1**·CB[8] and **P2**, leading to the interfacial formation of a supramolecular polymeric skin ( $\mathbf{P2}_{in} \cdot \mathbf{P1}_{out} \subset \text{CB[8]}$ ). The inner chloroform phase of the microdroplet can be evaporated, allowing the microcapsule skin to be visualized. As the droplet evaporates the diameter contracted, up to 120 s, at which point the spherical shape of the droplet became slightly distorted. As evaporation proceeded, wrinkles in the surface became visible, with these developing into marked creases and eventually folds. The appearance of wrinkling is used as evidence that an elastic polymer skin has formed at the interface of the droplet and we are no longer in a liquid-liquid regime. Upon further evaporation the droplet can no longer support the microcapsule skin, resulting in the top of the microcapsule collapsing onto the base, giving rise to sharp, irregular folds once dry (Fig. 1e). The observed collapse of the microcapsule, rather than ingress of the carrier fluid to replace the lost droplet media, is attributed to surfactant coating the capsule skin and acting as a barrier. Fluorescent microscopy of the microcapsule shell showed a bilayer of polymers that comprised the supramolecular self-assembled network. Green fluorescence from fluorescein-labelled **P1** can be clearly resolved on the outer layer of the polymeric shell, while the chloroform droplet-bound **P2** (Rhodamine B labelled, red) is completely localised at the inside face of the microcapsule (Fig. 1f). The absence of any fluorescence dispersed across either the droplet or carrier solvent (water) confirms the quantitative nature of this interfacial templating effect, with all functionalised copolymers localised within the resultant microcapsule skin.

To assess the significance of the supramolecular heteroternary complex, a number of control experiments were carried out. In the absence of CB[8], as shown in Fig. 2a, formation of stable microcapsules was not observed, rather any structures formed were observed to break, giving rise to flower-like polymer sheets. Similarly, microcapsule formation was not observed when employing the smaller macrocycle cucurbit[7]uril (CB[7]), which is capable of complexing only one  $MV^{2+}$  moiety, but not a second guest, preventing formation of a 1:1:1 heteroternary complex. In this case, copolymers **P1** and **P2** were no longer assembled at the chloroform-water droplet interface, but instead remained dispersed throughout the media as shown in Fig. 2b. Importantly, both of these control experiments show that the aggregation of supramolecular copolymers exclusively occurs at the droplet interface as a direct result of CB[8] heteroternary complex formation.

To further demonstrate the versatility of this interfacial approach to supramolecular microcapsule for-

mation, the inverse 'water-in-chloroform' microdroplets were prepared in the corresponding hydrophobic microfluidic flow focussing device. The nature of the continuous and discontinuous phases were reversed, with **P1** and CB[8] now confined to the aqueous droplet and **P2** located in the organic carrier fluid (1:5 v/v mixture of hexadecane in chloroform). As before, all polymeric materials localised at the microdroplet interface for supramolecular assembly, with the complementary fluorescence profile observed as highlighted in Fig. 1g; with **P1** now visible on the inner face and **P2** on the outside ( $P1_{in} \cdot P2_{out} \subset CB[8]$ ).

### Interfacial assembly of dendritic supramolecular capsules

To demonstrate how this multilayer microcapsule can be exploited for both cargo encapsulation and subsequent release with an external stimuli, such as UV light, a dendritic copolymer was designed and synthesised *via* RAFT copolymerisation of divinyl monomer, ethylene glycol dimethacrylate (EGDMA), containing

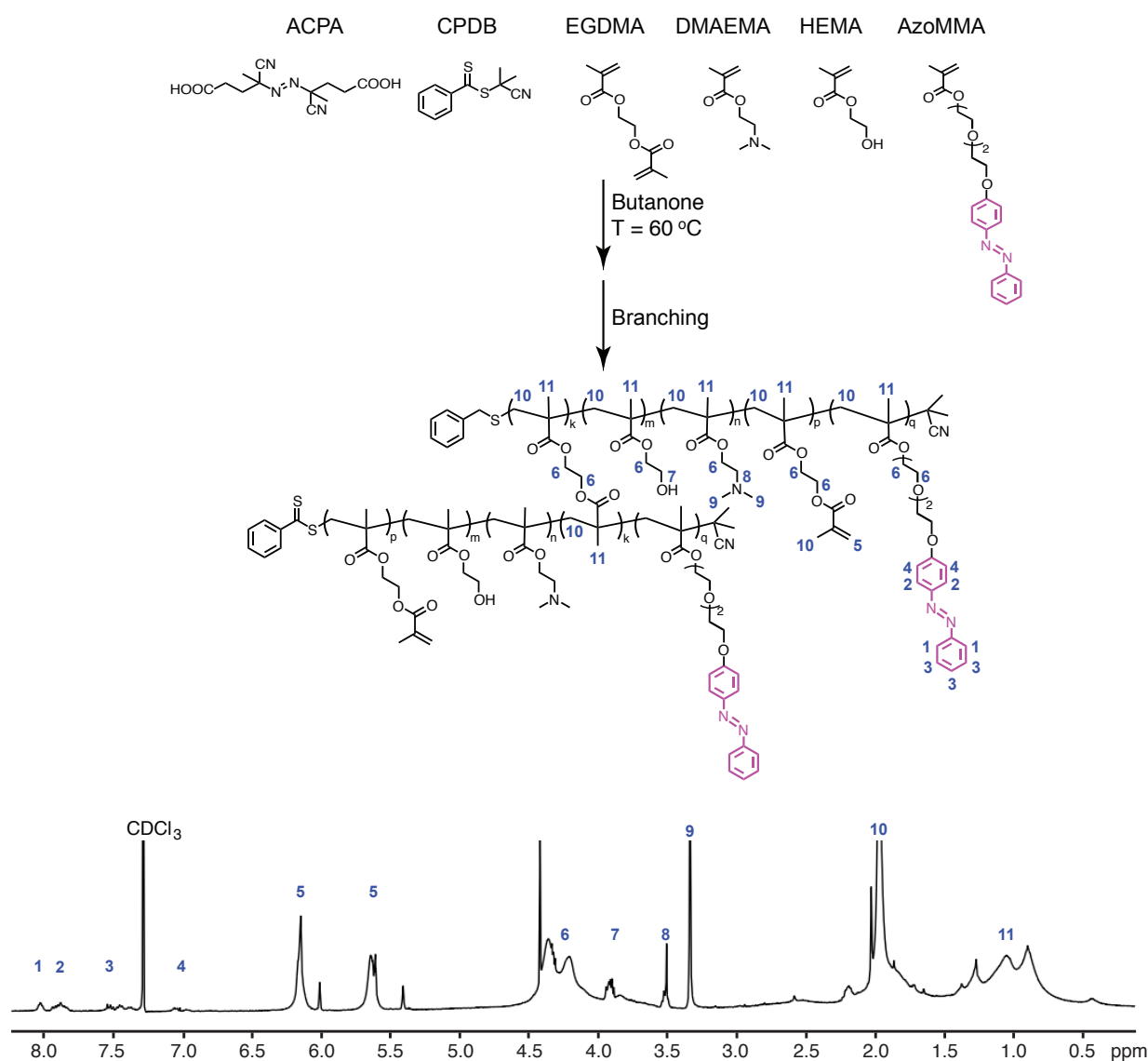


**Figure 3: Chemical structures and <sup>1</sup>H NMR spectrum of dendritic copolymer H1.** The dendritic copolymer (**H1**) was synthesised *via* RAFT copolymerisation of the divinyl monomer, ethylene glycol dimethacrylate (EGDMA) and incorporates azobenzene for photoresponsive complexation with CB[8]. The branching ratio is defined as the ratio of EGDMA units to all monomer units, as shown in Supplementary Equation 1.

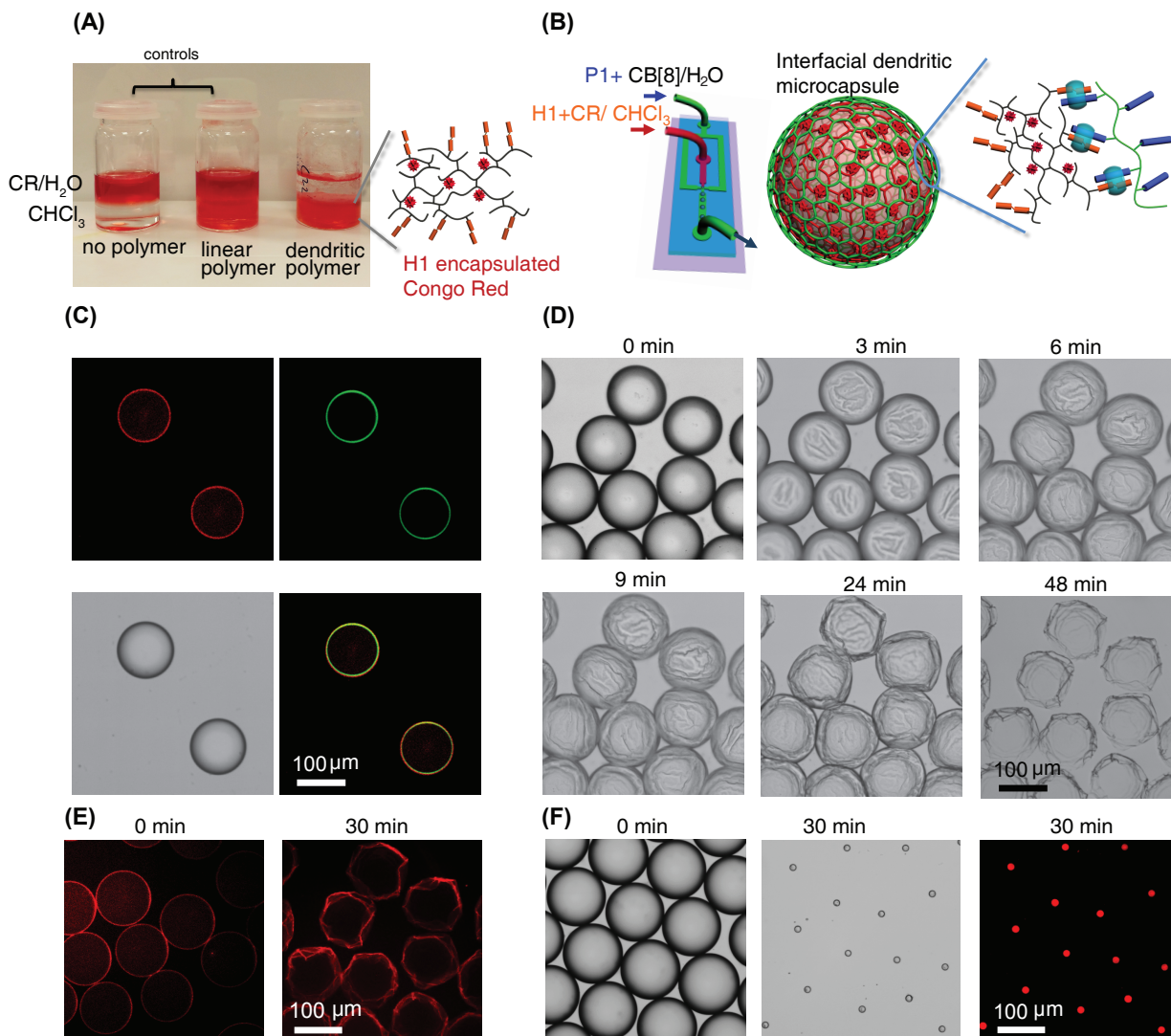


**Figure 4: Interfacial assembly of supramolecular dendritic microcapsules.** (a) Photograph of the entrapment of water-soluble Congo Red and its transfer into organic solvent by the dendritic copolymer, **H1**. (b) Schematic representation of the microdroplet generation process using a microfluidic flow focussing device, comprising an aqueous continuous phase containing CB[8] and **P1** intersecting a perpendicular flow of chloroform containing dendritic copolymer **H1** with entrapped Congo Red, to form chloroform-in-water microdroplets. (c) Fluorescence and optical micrographs of the highly monodisperse microdroplets formed, illustrating the interfacial assembly of an inner **H1** layer (entrapped Congo Red) and a **P1** outer layer (Fluorescein-tagged). (d) Bright field images of the formation of the microcapsule skin as the chloroform microdroplet evaporates, resulting in a collapsed capsule-like structure. (e) Fluorescence images of microcapsule formation verifying that Congo Red is entrapped within the microcapsule wall. (f) A control experiment in the absence of CB[8], confirmed that **P1** and **H1** no longer assemble at the interface of the droplets, but remain dispersed within the media to form dense polymer beads of **H1** upon evaporation, rather than a microcapsule.

a UV-responsive azobenzene-containing second guest for CB[8] (Fig. 3).

Two vinyl groups exist within the EGDMA monomer that can form a branch point under the right synthetic conditions, thus yielding a dendritic architecture (instead of a crosslinked network) using controlled/living free radical polymerisation<sup>47,48</sup>. Copolymerisation towards the dendritic polymer, poly(EGDMA-*co*-DMAEMA-*co*-HEMA-*co*-Azo), (**H1**) was monitored by THF GPC (refractive index detector, Supplementary Figure 3), which indicated a broadening of peaks between 1 h (PDI = 2.3) and 3 h (PDI = 4.2). Complete solubility (in THF) with concomitant peak broadening suggested that the major reaction pathway up to 3 h was the combination of growing polymer chains achieving a dendritic structure. The molecular weight of the purified polymer **H1** reached 41.8 kDa (PDI = 2.7) at

3 h without gelation (Supplementary Table 1). **H1** displayed a high branching ratio of 17.5% and contained 2.5 mol% of azobenzene guest, as calculated from the <sup>1</sup>H NMR spectrum (Fig. 3), indicating a highly branched structure formed from enhanced intermolecular coupling rather than chain growth. Here, the branching ratio is defined as the proportion of branched EGDMA monomers relative to the sum of all monomer units, including linear EGDMA, branched EGDMA, HEMA, DMAEMA and AzoMMA monomers (see Supplementary Equation 1 for calculation).

Dendritic copolymer **H1** was able to entrap hydrophilic small molecule 'cargo' on account of its unique three-dimensional nanoscale structure. Here, the fluorescent dye, Congo Red, was encapsulated (Fig. 4a) for subsequent studies. The dendritic copolymer is far superior in its ability to entrap small

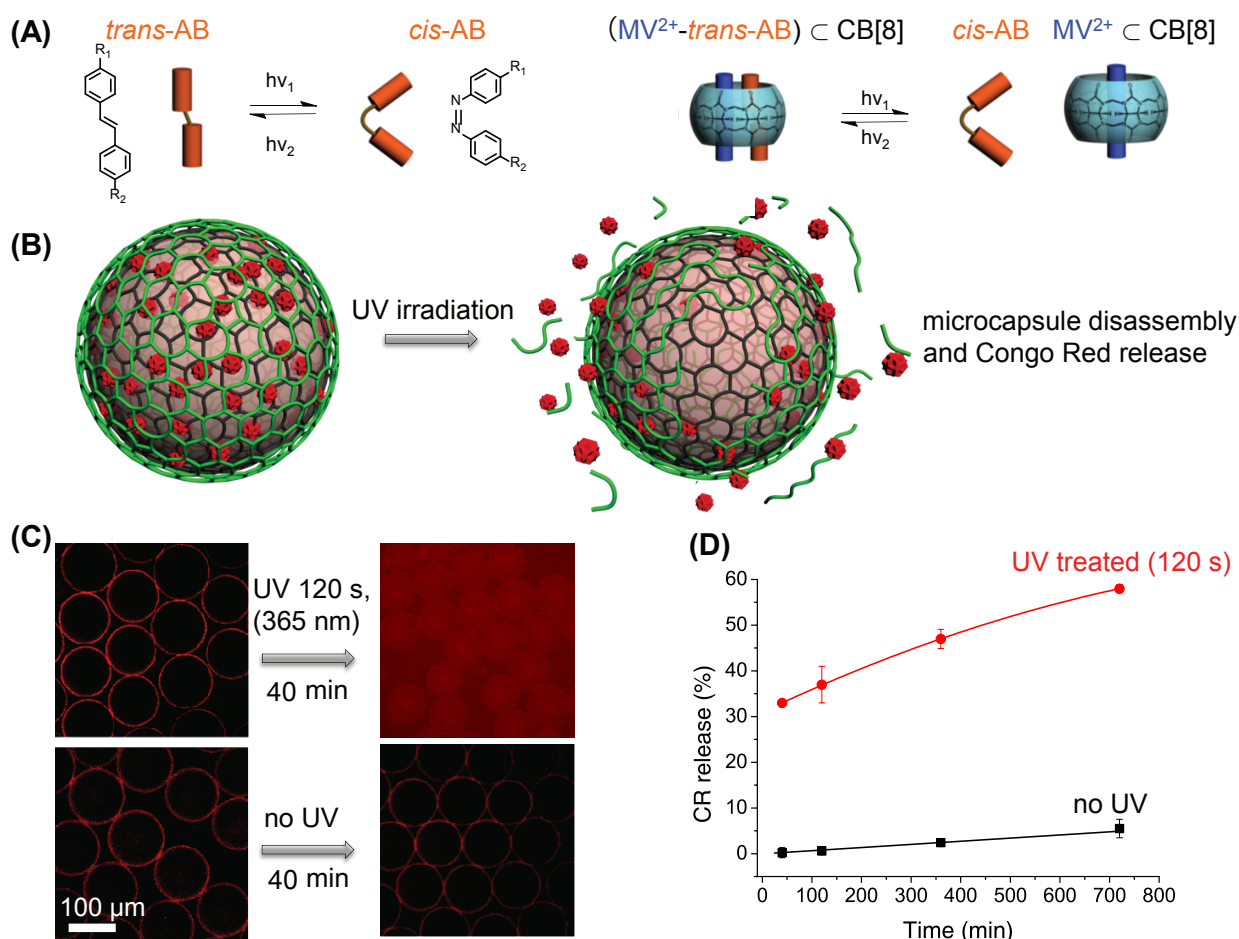


**Figure 5: Photo-triggered release of cargo from supramolecular dendritic microcapsules.** (a) UV light-driven photo-isomerisation of the azobenzene moiety can be used to disassemble the heteroternary supramolecular complex between MV, azobenzene and CB[8]. (b) Schematic representation of the triggered disassembly of the **H1**-containing microcapsule on exposure to 365 nm UV light with corresponding release of the entrapped Congo Red molecular cargo. (c) Fluorescence micrographs showing release of the entrapped Congo Red from **H1**·**P1**⊂CB[8] microcapsules, with and without initial UV irradiation. (d) Time-resolved Congo Red release profiles from **H1**·**P1**⊂CB[8] microcapsules as a function of initial UV irradiation for 120 s.

molecules over its linear analogue as demonstrated by a control experiment using poly(MMA-*co*-DMAEMA-*co*-HEMA-*co*-Azo), with a comparable molecular weight,  $M_w = 38.1$  kDa and PDI = 1.4. The absorption studies concluded that the dendritic **H1** can entrap 4.1 times more Congo Red into a hydrophobic environment than its linear analogue, at the same concentration of copolymer (Fig. 4a, Supplementary Table 2 and Supplementary Figure 5). To fabricate dendritic supramolecular microcapsules *via* interfacial assembly, monodisperse chloroform microdroplets containing Congo Red entrapped within **H1** were generated in an aqueous continuous phase, which contained **P1** and CB[8] (Fig. 4b). It is worth noting that although **H1** does not contain a fluorescent tag, the entrapped fluorescent dye, Congo Red, was used to directly monitor polymer assembly at the droplet interface. It was observed by fluorescent microscopy that interfacial assembly indeed occurred at the droplet interface (Fig. 4c), leading to supramolecular microcapsule formation upon subsequent evaporation of the chloroform, with the formation of creases and folds upon collapse of the flexible polymer skin (Fig. 4d and e). Microdroplets generated in the absence of CB[8] did not lead to robust aggrega-

tion at the droplet interface leading to the formation of dense polymer beads of **H1** upon evaporation (Fig. 4f).

The CB[8] heteroternary complex, beyond providing a means for directing self-assembly and locking together the multilayer capsule skin, also imparts inherent stimuli responsiveness that can be employed to trigger the release of encapsulants. This is demonstrated here through photoisomerisation of the azobenzene moiety on **H1**, destabilising the heteroternary complex and leading to capsule disassembly. As synthesised, the azobenzene group on **H1** exists primarily as the *trans*-isomer, however, upon irradiation with UV light (365 nm) it photoisomerises into the *cis*-isomer (Fig. 5a left)<sup>49</sup>, with the photo-stationary state expected to contain up to 80% of the *cis*-isomer in the presence of CB[8]<sup>33</sup>. This conformational change (Fig. 5a right) does not allow for heteroternary complexation within the cavity of CB[8]. This leads to significant disassembly of the microcapsule skin, resulting in a rapid increase in porosity and liberating individual dendritic polymer, allowing the Congo Red to partition into the aqueous phase over time (Fig. 5b). Consequently, UV stimulus-controlled release of the Congo Red cargo from  $\mathbf{P1}_{out} \cdot \mathbf{H1}_{in} \cdot \text{CR} \subset \text{CB}[8]$  microcapsules

was achieved after brief exposure to UV light (120 s), which could be observed in the surrounding aqueous media over time. To avoid any evaporation of the chloroform from the microcapsules, they were collected in a covered vial while the release behaviour of Congo Red was measured. Our experimental results showed that exposure to UV light for 120 s led to facile disruption of the capsule giving rise to a steady release of the fluorescent cargo, with 33% released in 40 min. In contrast, a negligible release of cargo was observed for the control experiment over a similar timescale, with Congo Red remaining localised within the microcapsule skin (Fig. 5c). Fig. 5d depicts the long-term release profile of Congo Red from the dendritic supramolecular microcapsules with and without initial UV-irradiation for 120 s. Over 12 h microcapsules that had been irradiated slowly released up to 60% of their cargo, compared to only 5% for the unexposed control.

## Discussion

We have shown a simple and robust means of directing the assembly of supramolecular polymeric materials at a hydrophilic/hydrophobic droplet interface to form an encapsulating skin. The interfacial assembly process critically relies upon the supramolecular heteroternary host-guest complex formed between CB[8] and suitable guest moieties on the constituent copolymers. This bi-layer assembly of hydrophilic and hydrophobic copolymers will uniquely allow for the expression of orthogonal chemical functionalities at the inner and outer faces of the microcapsule, enabling greater control over the properties of the microcapsule.

By moving from a nanoparticle-mediated microcapsule assembly process to one driven by interfacial assembly of copolymers we retain the advantages of supramolecular assembly, but benefit from the diversity of synthesised polymeric materials, allowing for fine control over the properties and function of the microcapsules, including wall thickness, permeability and an expanded toolset for cargo release. By exploiting a dendritic copolymer small molecules were successfully encapsulated, overcoming the restriction of molecular weight. Combined with the ability to segregate and store water-soluble and oil-soluble cargo within a single structure, this extends the range of potential application into new areas, such as drug delivery. The incorporation of azobenzene as a polymer-bound guest for CB[8] enabled the introduction of a controllable release valve into the microcapsule skin, demonstrating remote manipulation of microcapsule properties under mild conditions.

Importantly, these interfacially-assembled bi-layer microcapsules afford a unique platform with which one could quantitatively investigate the mechanism and kinetics of self-assembly at liquid-liquid or soft matter interfaces, of great relevance in all biological systems<sup>50,51</sup>.

## Methods

### Materials

Methyl methacrylate, hydroxyethylmethacrylate, ethylene glycol dimethacrylate, N,N-dimethylaminoethyl methacrylate and acrylic acid monomers were

purchased from Sigma-Aldrich and were passed through a column of silica gel and purged with high purity nitrogen for 1 h prior to use. Fluorescein *o*-acrylate (FOA) and 2-naphthyl isocyanate were purchased from Alfa Aesar. 2-Cyano-2-propyl benzodithioate, 4,4-azobis(4-cyanovaleric acid), Rhodamine B isothiocyanate, Congo Red (analytical standard), polyvinyl acetate (PVA,  $M_w$ =13-23 kDa) and 2-butanone (HPLC grade) were purchased from Sigma-Aldrich. MV-styrene, the azobenzene monomer and CB[8] were synthesised as previously reported (See Supplementary Methods). Solvents and reagents were used without further purification unless otherwise stated.

### Preparation of poly(HEMA-*co*-StMV-*co*-FOA) (P1)

Poly(HEMA-*co*-StMV-*co*-FOA) was synthesised *via* RAFT polymerisation using the unmodified chain transfer agent 2-cyano-2-propyl benzodithioate. To a two-neck round bottom flask were added 2-cyano-2-propyl benzodithioate (CPBD, 22.1 mg, 0.1 mmol, 1 eq.), hydroxyethylmethacrylate (HEMA, 1.3 g, 10 mmol, 100 eq.), MV-styrene (StMV, 0.9 g, 2 mmol, 20 eq.) and FOA (38.6 mg, 0.1 mmol, 1 eq.) in a 50:50 wt% mixture of aqueous methanol (6 ml). Oxygen was removed by bubbling argon through the solution for 20 min, followed by the subsequent addition of 4,4-azobis(4-cyanovaleric acid) (ACPA, 14 mg, 0.05 mmol, 0.5 eq.). The flask was then immersed in a preheated oil bath (65 °C) and the solution stirred at 400 rpm for 24 h. The resultant polymer was dialysed in water through a MWCO 6,000-8,000 membrane and freeze dried. The formed polymer was characterised to give  $M_w$  = 21 kDa, PDI = 1.2 from GPC, HEMA:StMV = 100:23 from <sup>1</sup>H NMR (Supplementary Figure 1).

### Preparation of poly(MMA-*co*-AA-*co*-HEMA-Np) (P2)

Poly(MMA-*co*-AA-*co*-HEMA-Np) was synthesised *via* RAFT polymerisation using the unmodified chain transfer agent CPBD. To a two-necked round bottom flask were added CPBD (22.1 mg, 0.1 mmol, 1 eq.), methyl methacrylate (MMA, 1.0 g, 10 mmol, 100 eq.), HEMA (0.325 g, 2.5 mmol, 25 eq.) and acrylic acid (AA, 0.18 g, 2.5 mmol, 25 eq.) in 2-butanone (8 ml). Oxygen was removed by bubbling argon through the solutions for 20 min, followed by the subsequent addition of ACPA (14 mg, 0.05 mmol, 0.5 eq.). The flask was immersed in a preheated oil bath (65 °C) and the solution stirred at 400 rpm for 24 h. The polymer was precipitated into cold hexane and finally dried *in vacuo* at 50 °C. The resultant polymer was then subsequently functionalised with naphthalene isocyanate (10 % molar ratio) and Rhodamine B isothiocyanate (1 % molar ratio). The final polymer was characterised to give  $M_w$  = 16 kDa, PDI = 1.2 from GPC, MMA: HEMA: AA: Np = 100 : 30 : 27.2 : 4.5 from <sup>1</sup>H NMR (Supplementary Figure 2).

### Preparation of dendritic poly(EGDMA-*co*-DMAEMA-*co*-HEMA-*co*-Azo) (H1)

Poly(EGDMA-*co*-DMAEMA-*co*-HEMA-*co*-Azo) was synthesised *via* RAFT polymerisation using the unmodified chain transfer agent CPBD. To a two-neck round

bottom flask were added CPBD (22.1 mg, 0.1 mmol, 1 eq.), EGDMA (3.98 g, 20 mmol, 200 eq.), HEMA (0.35 g, 2.5 mmol, 25 eq.), DMAEMA (0.39 g, 2.5 mmol, 25 eq.) and AzoMMA (199 mg, 0.5 mmol, 5 eq.) in 2-butanone (12 ml, [EGDMA] = 1.25 M). Oxygen was removed by bubbling argon through the solutions for 20 min, followed by the subsequent addition of ACPA (14 mg, 0.05 mmol, 0.5 eq.). The flask was immersed in a preheated oil bath (60 °C) and the solution stirred at 400 rpm for the desired reaction time. The resultant polymer was precipitated into cold hexane and dried in *vacuo* at room temperature. The purified polymer was characterised to give  $M_w = 41.8$  kDa, PDI = 2.7 from GPC (Supplementary Table 1 and Supplementary Figure 3), linear EGDMA: branched EGDMA: HEMA: DMAEMA: AzoMMA = 35: 17.5: 21: 24: 2.5 from  $^1\text{H}$  NMR (Fig. 3 and Supplementary Equation 1).

### Encapsulation of Congo Red

Typically, 2 mL of an aqueous solution of Congo Red (CR, 0.01 mg/ml) was mixed with 2 mL of a chloroform solution containing the dendritic polymer **H1** in a glass vial and the mixture was shaken for 24 h to ensure the two phases were sufficiently mixed. The two phases were allowed to separate and the lower chloroform layer transferred to a cuvette and its absorption spectrum recorded. In all experiments, the concentration of Congo Red in the aqueous phase was in great excess to ensure the maximum loading capacity ( $C_{\text{load}}$ ) within **H1** was achieved. The amount of encapsulated dye was determined quantitatively from the absorption spectrum (CR  $\lambda_{\text{max}} = 498$  nm). Detailed results are presented in Supplementary Table 2 for the ability of the dendritic polymer **H1** to encapsulate Congo Red compared to the equivalent linear polymer, poly(MMA-co-DMAEMA-co-HEMA-co-Azo), as a control (see SI). The calibration of absorbance against Congo Red concentration is shown in Supplementary Figure 4.

### Fabrication and characterisation of the microcapsules

All microfluidic chips used in this work were manufactured from silica and purchased fully assembled from Dolomite. To produce monodisperse oil-in-water microdroplets a hydrophilic flow-focussing microfluidic chip was employed (100  $\mu\text{m}$  channel depth, 3000158 Droplet Junction Chip) and to ensure a hydrophilic microchannel, the chip was pretreated with a sequential layer-by-layer deposition of polyallylamine hydrochloride (PAH) and poly(sodium styrene sulfonate) (PSS) polyelectrolytes. The hydrophobic phase (chloroform) and the hydrophilic aqueous phase were injected into the microfluidic device *via* two syringe pumps (PHD, Harvard Apparatus) with controlled flow rates. The continuous aqueous phase was prepared by dissolving CB[8] and **P1** in a 1 wt% polyvinylalcohol solution, while the discontinuous phase comprised of a 4:1 *v/v* mix of chloroform and HFE-7500 (3M), into which **P2** was dissolved. Microdroplet formation was initiated by first pumping the aqueous continuous phase into the device at the rate of 400  $\mu\text{L/h}$ , to fill the appropriate channels, followed by the discontinuous oil phase into the middle channel of the flow focussing device at 200  $\mu\text{L/h}$ . At

these flow rates, the oil flow was periodically sheared at the flow focus to form microdroplets within an aqueous carrier flow. For a typical experiment, the concentrations of MV, Np, and CB[8] were all 30  $\mu\text{M}$ . Once formed microdroplets were collected on the surface of glass slide for further study.

To prepare the inverse water-in-oil microdroplet, the equivalent hydrophobic flow-focussing microfluidic chip was employed (190  $\mu\text{m}$  etch depth, 3000437 Droplet Junction Chip). As before the two phases were injected into the microfluidic device *via* syringe pumps with precise control over the flow rate. The discontinuous phase was prepared by dissolving copolymer **P1** and CB[8] in water, while the continuous oil phase comprised a 1:5 *v/v* mixture of chloroform in hexadecane, into which **P2** was dissolved. To prevent fusion of the prepared microdroplets, 2 wt% of the surfactant Span 80 was further added to the continuous phase. As before, the continuous phase (oil) was first pumped into the device at the rate of 400  $\mu\text{L/h}$  to fill the appropriate channels followed by the aqueous discontinuous phase at 200  $\mu\text{L/h}$ . At these flow rates, the aqueous flow was periodically sheared at the flow focus to form water-in-oil microdroplets. In a typical experiment, the concentrations of MV, Np, and CB[8] were all 30  $\mu\text{M}$ . Once formed, microdroplets were collected on the surface of glass slide for further study.

Congo Red loaded microdroplets, formed from dendritic polymer **H1**, were templated *via* an oil-in-water microdroplet motif and as such required a hydrophilic microfluidic channel. As before, the continuous aqueous phase was prepared by dissolving CB[8] and **P1** in 1 wt% polyvinylalcohol solution, however the discontinuous phase contained **H1** carrying Congo Red dissolved in chloroform exclusively. Microdroplet formation was initiated by first pumping the aqueous continuous phase into the device at the rate of 400  $\mu\text{L/h}$ , to fill the appropriate channels, followed by the discontinuous oil phase into the middle channel of the flow focussing device at 200  $\mu\text{L/h}$ . At these flow rates, the oil flow was periodically sheared at the flow focus to form microdroplets within an aqueous carrier flow. In a typical experiment, the concentrations of MV, Azo, and CB[8] were all 150  $\mu\text{M}$ . Once formed, microdroplets were collected on the surface of glass slide for further study.

### UV-triggered microcapsule disassembly and cargo release

To investigate triggered disassembly of the supramolecular crosslinks leading to microcapsule rupture the fluorescent dye, Congo Red, was employed to probe release of encapsulant from the microcapsule. Throughout the release experiment the vial was kept in the dark and at room temperature to minimize reconversion back to the *trans* isomer. Additionally, the presence of PVA in the carrier solution stabilized the chloroform droplets throughout the release studies. The dendritic polymer (**H1**) was used to entrap Congo Red as described above, with 3.64 mg polymer **H1** found to contain 1.82  $\mu\text{g}$  of Congo Red (0.05 wt% loading) and then employed in the preparation of microcapsules, with Congo Red encapsulated

within the microcapsule skin. After washing the formed microcapsules three times with water to remove any free dye, 2.5 ml of water was added into the vial. The prepared microcapsules were exposed to a UV light source using a LZC-ORG photo-reactor with both 350 nm wavelength lamps for 2 min. Aliquots of the aqueous phase were collected at set intervals after the initial UV exposure (40, 120, 360 and 720 min) and the absorption spectrum recorded. The release profile of Congo Red from the microcapsules after UV exposure and for a control are given in Supplementary Table 3 and Fig. 5.

### Instrumentation

$^1\text{H}$  NMR spectra (400 MHz) were collected on a Bruker Avance QNP 400 MHz Ultrashield spectrometer, equipped with a 5-mm BBO ATM probe with a z-gradient. UV/visible spectra were recorded on a Varian Cary 4000 UV/visible spectrophotometer. Microscopic images and fluorescence images were obtained using an Olympus IX81 inverted optical microscope coupled with a camera of Andor Technology EM-CCD iXonEM+ DU 897. Photo-irradiation was performed on a LZC-ORG photoreactor with both 365 nm wavelength lamps. Titration experiments were carried out on a ITC200 from Microcal Inc. Weight average molecular weight ( $M_w$ ), number average molecular weight ( $M_n$ ) and polydispersity ( $M_w/M_n$ ) were obtained by aqueous or THF GPC. The aqueous GPC setup consisted of a Shodex OHpak SB column, connected in series with a Shimadzu SPD-M20A prominence diode array detector, a Wyatt DAWN HELEOS multi-angle light scattering detector and a Wyatt Optilab rEX refractive index detector. The THF GPC setup consisted of two 30 cm PLgel Mixed-C columns in series, eluted using THF and calibrated against a series of twelve near-monodisperse PMMA standards ( $M_p$  from 690 to 1,944,000  $\text{g mol}^{-1}$ ). The polymers were analysed in THF at a concentration of 5.0 mg/ml. All calibrations and analysis were performed at 35 °C and a flow rate of 1 ml/min.

### Acknowledgements

This work was supported by the Engineering Physical Sciences Research Council, Institutional Sponsorship 2012-University of Cambridge EP/K503496/1 and the Translational Grant EP/H046593/1; Dr Yu Zheng and Dr Richard M. Parker were also funded from the Starting Investigator grant ASPIRe (No. 240629) from the European Research Council and the Isaac Newton Trust research grant No. 13.7(c). The authors would like to acknowledge Dr Roger J. Coulston and Dr Jing Zhang for their detailed and helpful discussion to this manuscript.

### Author Contributions

Y.Z. and Z.Y. contributed equally to this work. Y.Z. designed and synthesised polymers, prepared figures, analysed data and wrote the paper; Z.Y. performed microfluidic experiments, prepared figures and analysed data; R.M.P prepared figures and wrote the paper; Y.W. analysed data, prepared figures and wrote

the paper. C.A. and O.A.S. supervised the experimental design, analysed data and wrote the paper. All authors were involved in fundamental discussions, preliminary and supporting studies and critical revisions of the manuscript.

**Competing financial interests:** The authors declare no competing financial interests

### References

- [1] Huang, X., Li, M., Green, D. C., Williams, D. S., Patil, A. J., and Mann, S. Interfacial assembly of protein-polymer nano-conjugates into stimulus-responsive biomimetic protocells. *Nat. Commun.* **4**, 2239 (2013).
- [2] Gröschel, A. H., Walther, A., Löbbling, T. I., Schacher, F. H., Schmalz, H., and Müller, A. H. E. Guided hierarchical co-assembly of soft patchy nanoparticles. *Nature* **503**, 247–51 (2013).
- [3] Bain, C. D., Troughton, E. B., Tao, Y. T., Evall, J., Whitesides, G. M., and Nuzzo, R. G. Formation of monolayer films by the spontaneous assembly of organic thiols from solution onto gold. *J. Am. Chem. Soc.* **111**, 321–35 (1989).
- [4] Lin, Y., Skaff, H., Böker, A., Dinsmore, A. D., Emrick, T., and Russell, T. P. Ultrathin cross-linked nanoparticle membranes. *J. Am. Chem. Soc.* **125**, 12690–1 (2003).
- [5] Genzer, J. and Kirill, E. Creating Long-Lived Superhydrophobic Polymer Surfaces Through Mechanically Assembled Monolayers. *Science* **290**, 2130–3 (2000).
- [6] Zhao, B. and Brittain, W. J. Polymer brushes: surface-immobilized macromolecules. *Prog. Polym. Sci.* **25**, 677–710 (2000).
- [7] Skaff, H., Lin, Y., Tangirala, R., Breitenkamp, K., Böker, A., Russell, T. P., and Emrick, T. Crosslinked Capsules of Quantum Dots by Interfacial Assembly and Ligand Crosslinking. *Adv. Mater.* **17**, 2082–6 (2005).
- [8] Lin, Y., Skaff, H., Emrick, T., Dinsmore, A. D., and Russell, T. P. Nanoparticle assembly and transport at liquid-liquid interfaces. *Science* **299**, 226–9 (2003).
- [9] Russell, J. T., Lin, Y., Böker, A., Su, L., Carl, P., Zettl, H., He, J., Sill, K., Tangirala, R., Emrick, T., Littrell, K., Thiyagarajan, P., Cookson, D., Fery, A., Wang, Q., and Russell, T. P. Self-assembly and cross-linking of bionanoparticles at liquid-liquid interfaces. *Angew. Chem. Int. Ed.* **44**, 2420–6 (2005).
- [10] Theberge, A. B., Courtois, F., Schaerli, Y., Fischlechner, M. Abell, C. and Hollfelder, F., and Huck, W. T. S. Microdroplets in microfluidics: an evolving platform for discoveries in chemistry and biology. *Angew. Chem. Int. Ed.* **49**, 5846–68 (2010).
- [11] Tumarkin, E., Kumacheva, E. Microfluidic generation of microgels from synthetic and natural polymers. *Chem. Soc. Rev.* **38**, 2161–8 (2009).
- [12] Stephenson, G., Parker, R. M., Lan, Y., Yu, Z. Y., Scherman, O. A. and Abell, C. Supramolecular

- colloidosomes: fabrication, characterisation and triggered release of cargo. *Chem Commun.* **50**, 7048–51 (2014).
- [13] Zhou, S., Fan, J., Datta, S. S., Guo, M., Guo, X., and Weitz, D. A. Thermally Switched Release from Nanoparticle Colloidosomes. *Adv. Funct. Mater.* **23**, 5925–9 (2013).
- [14] Abbaspourrad, A., Carroll, N. J., Kim, S.-H., and Weitz, D. A. Polymer microcapsules with programmable active release. *J. Am. Chem. Soc.* **135**, 7744–50 (2013).
- [15] Kim, S.-H., Park, J.-G., Choi, T. M., Manoharan, V. N., and Weitz, D. A. Osmotic-pressure-controlled concentration of colloidal particles in thin-shelled capsules. *Nat. Commun.* **5**, 3068 (2014).
- [16] Jiao, D., Geng, J., Loh, X. J., Das, D., Lee, T.-C., and Scherman, O. A. Supramolecular peptide amphiphile vesicles through host-guest complexation. *Angew. Chem. Int. Ed.* **51**, 9633–7 (2012).
- [17] Kim, E., Kim, D., Jung, H., Lee, J., Paul, S., Selvapalam, N., Yang, Y., Lim, N., Park, C. G., and Kim, K. Facile, template-free synthesis of stimuli-responsive polymer nanocapsules for targeted drug delivery. *Angew. Chem. Int. Ed.* **49**, 4405–8 (2010).
- [18] Li, H., Bian, Z., Zhu, J., Zhang, D., Li, G., Huo, Y., Li, H., and Lu, Y. Mesoporous titania spheres with tunable chamber structure and enhanced photocatalytic activity. *J. Am. Chem. Soc.* **129**, 8406–7 (2007).
- [19] Amstad, E., Kim, S.-H., and Weitz, D. A. Photo- and thermoresponsive polymersomes for triggered release. *Angew. Chem. Int. Ed.* **51**, 12499–503 (2012).
- [20] Peyratout, C. S. and Dähne, L. Tailor-made polyelectrolyte microcapsules: from multilayers to smart containers. *Angew. Chem. Int. Ed.* **43**, 3762–83 (2004).
- [21] Becker, A. L., Johnston, A. P. R., and Caruso, F. Layer-by-layer-assembled capsules and films for therapeutic delivery. *Small* **6**, 1836–52 (2010).
- [22] De Cock, L. J., De Koker, S., De Geest, B. G., Grooten, J., Vervaet, C., Remon, J. P., Sukhorukov, G. B., and Antipina, M. N. Polymeric multilayer capsules in drug delivery. *Angew. Chem. Int. Ed.* **49**, 6954–73 (2010).
- [23] Utada, A. S., Lorenceau, E., Link, D. R., Kaplan, P. D., Stone, H. A., and Weitz, D. A. Monodisperse double emulsions generated from a microcapillary device. *Science* **308**, 537–41 (2005).
- [24] Gao, F., Su, Z.-G., Wang, P., and Ma, G.-H. Double emulsion templated microcapsules with single hollow cavities and thickness-controllable shells. *Langmuir* **25**, 3832–8 (2009).
- [25] Hermanson, K., Huemmerich, D., Scheibel, T., and Bausch, A. R. Engineered Microcapsules Fabricated from Reconstituted Spider Silk. *Adv. Mater.* **19**, 1810–5 (2007).
- [26] Thompson, K. L., Armes, S. P., Howse, J. R., Ebbens, S., Ahmad, I., Zaidi, J. H., York, D. W., and Burdis, J. A. Covalently Cross-Linked Colloidosomes. *Macromolecules* **43**, 10466–74 (2010).
- [27] Duan, H., Wang, D., Sobal, N. S., Giersig, M., Kurth, D. G., and Möhwald, H. Magnetic Colloidosomes Derived from Nanoparticle Interfacial Self-Assembly. *Nano Lett.* **5**, 949–52 (2005).
- [28] Wang, W., Zhang, M. J., Xie, R., Ju, X. J., Yang, C., Mou, C. L., Weitz, D. A. and Chu, L. Y. Hole-shell microparticles from controllably evolved double emulsions. *Angew. Chem. Int. Ed.* **52**, 8084–7 (2013).
- [29] Abbaspourrad, A., Carroll, N. J., Kim, S. H. and Weitz, D. A. Polymer microcapsules with programmable active release. *J. Am. Chem. Soc.* **135**, 7744–50 (2013).
- [30] Tsuda, N., Ohtsubo, T., and Fujii, M. Preparation of self-bursting microcapsules by interfacial polymerization. *Adv. Powder. Tech.* **23**, 724–30 (2012).
- [31] Kobašlija, M. and McQuade, D. T. Polyurea Microcapsules from Oil-in-Oil Emulsions via Interfacial Polymerization. *Macromolecules* **39**, 6371–5 (2006).
- [32] Levy, M. C. and Andry, M. C. Microcapsules prepared through interfacial cross-linking of starch derivatives. *Int. J. Pharm.* **62**, 27–35 (1990).
- [33] del Barrio, J., Horton, P. N., Lairez, D., Lloyd, G. O., Toprakcioglu, C., and Scherman, O. A. Photocontrol over cucurbit[8]uril complexes: stoichiometry and supramolecular polymers. *J. Am. Chem. Soc.* **135**, 11760–3 (2013).
- [34] Liu, Y., Yu, Y., Gao, J., Wang, Z., and Zhang, X. Water-Soluble Supramolecular Polymerization Driven by Multiple Host-Stabilized Charge-Transfer Interactions. *Angew. Chem. Int. Ed.* **122**, 6726–9 (2010).
- [35] Rauwald, U. and Scherman, O. A. Supramolecular block copolymers with cucurbit[8]uril in water. *Angew. Chem. Int. Ed.* **47**, 3950–3 (2008).
- [36] Appel, E. A., Biedermann, F., Rauwald, U., Jones, S. T., Zayed, J. M., and Scherman, O. A. Supramolecular cross-linked networks via host-guest complexation with cucurbit[8]uril. *J. Am. Chem. Soc.* **132**, 14251–60 (2010).
- [37] Appel, E. A., Loh, X. J., Jones, S. T., Biedermann, F., Dreiss, C. a., and Scherman, O. A. Ultrahigh-water-content supramolecular hydrogels exhibiting multistimuli responsiveness. *J. Am. Chem. Soc.* **134**, 11767–73 (2012).
- [38] Lan, Y., Wu, Y., Karas, A., and Scherman, O. A. Photoresponsive Hybrid Raspberry-Like Colloids Based on Cucurbit[8]uril Host-Guest Interactions. *Angew. Chem. Int. Ed.* **126**, 2166–9 (2014).
- [39] Zhang, J., Coulston, R. J., Jones, S. T., Geng, J., Scherman, O. A., and Abell, C. One-step fabrication of supramolecular microcapsules from microfluidic droplets. *Science* **335**, 690–4 (2012).
- [40] Ko, Y. H., Kim, E., Hwang, I., and Kim, K. Supramolecular assemblies built with host-stabilized charge-transfer interactions. *Chem. Commun.* **13**, 1305–15 (2007).
- [41] Isaacs, L. Cucurbit[n]urils: from mechanism to structure and function *Chem. Commun.* **6**, 619–29 (2009).

- [42] Hecht, S. and Frechet, J. M. J. Dendritic Encapsulation of Function : Applying Nature's Site Isolation Principle from Biomimetics to Materials Science. *Angew. Chem. Int. Ed.* **40**, 74–91 (2001).
- [43] Patri, A. K., Majoros, I. J., and Baker, J. R. Dendritic polymer macromolecular carriers for drug delivery. *Curr. Opin. Chem. Biol.* **6**, 466–471 (2002).
- [44] Geng, J., Jiao, D., Rauwald, U., and Scherman, O. A. An Aqueous Supramolecular Side-Chain Polymer Designed for Molecular Loading. *Aust. J. Chem.* **63**, 627–30 (2010).
- [45] Loh, X. J., del Barrio, J., Lee, T.-C., and Scherman, O. A. Supramolecular polymeric peptide amphiphile vesicles for the encapsulation of basic fibroblast growth factor. *Chem. Commun.* **50**, 3033–5 (2014).
- [46] Rauwald, U., Biedermann, F., Deroo, S., Robinson, C. V. and Scherman, O. A. Correlating solution binding and ESI-MS stabilities by incorporating solvation effects in a confined cucurbit[8]uril system. *J. Phys. Chem. B.* **114**, 8606–15 (2010).
- [47] Zheng, Y., Cao, H., Newland, B., Dong, Y., Pandit, A., and Wang, W. 3D single cyclized polymer chain structure from controlled polymerization of multi-vinyl monomers: beyond Flory-Stockmayer theory. *J. Am. Chem. Soc.* **133**, 13130–7 (2011).
- [48] Zhao, T., Zheng, Y., Poly, J., and Wang, W. Controlled multi-vinyl monomer homopolymerization through vinyl oligomer combination as a universal approach to hyperbranched architectures. *Nat. Commun.* **4**, 1873 (2013).
- [49] Tian, F., Jiao, D., Biedermann, F., and Scherman, O. A. Orthogonal switching of a single supramolecular complex. *Nat. Commun.* **3**, 1207 (2012).
- [50] Appel, E. A., Koutsioubas, A., Forster, R. A., Toprakcioglu, C., and Scherman, O. A. Activation Energies Control Macroscopic Properties of Physically Crosslinked Materials. *Angew. Chem. Int. Ed.* **38**, 10038–43 (2014).
- [51] Yang, H., Yuan, B., Zhang, X., and Scherman, O. A. Supramolecular Chemistry at Interfaces: Host-Guest Interactions for Fabricating Multifunctional Biointerfaces. *Acc. Chem. Res.* **47**, 2106–15 (2014).